

Inexpensive Optimized $\text{Cu}_2\text{ZnSnS}_4$ Absorption Layer Elaborated with a Homemade SILAR Method

B. Benmazouza^{1,*}, T. Sahraoui¹, M. Adnane¹, N. Hamamousse², A. Djelloul^{3,†}, Y. Larbah⁴, L. Benharrat³

¹ LMESM, Département de Technologie des Matériaux, Faculté de Physique, Université des Sciences et de la Technologie d'Oran Mohamed Boudiaf USTO-MB, BP 1505, El M'naouer, 31000 Oran Algérie

² LEPSM, Département de Technologie des Matériaux, Faculté de Physique, Université des Sciences et de la Technologie d'Oran Mohamed Boudiaf USTO-MB, BP 1505, El M'naouer, 31000 Oran Algérie

³ Centre de Recherche en Technologie des Semi-Conducteurs pour l'Energétique 'CRTSE', 02 Bd Frantz Fanon, BP 140, 7 Merveilles, Alger, Algérie

⁴ Spectrometry Department, Nuclear Research Center of Algiers-CRNA, 02 Bd. Frantz Fanon BP, 399 Algiers, Algeria

(Received 10 January 2023; revised manuscript received 18 April 2023; published online 27 April 2023)

In this study, $\text{Cu}_2\text{ZnSnS}_4$ (CZTS) thin films were synthesized on glass substrates by using homemade successive ionic layer adsorption and reaction (SILAR) method. Copper (II) Chloride (CuCl_2), Zinc (II) Chloride (ZnCl_2), Tin (II) Chloride (SnCl_2) were used as a cationic precursors and Thiourea ($\text{CS}(\text{NH}_2)_2$) was used as precursor for anions. De-ionized (DI) water was taken as the solvent for both precursors. Few drops of ammonia were added to both solutions in order to ensure the adsorption on the glass substrate. The deposited films were annealed at 200 °C for 1 h in air atmosphere and characterized by X-rays diffraction (XRD), field emission scanning electron microscopy (FESEM), atomic force microscopy (AFM), ultraviolet-visible (UV-Vis) spectrophotometry and dielectric spectroscopy. The structural characterization using XRD revealed the formation of the kesterite phase with preferential orientation along (112) plane. Morphological observations from SEM and AFM exhibited uniform and homogenous CZTS thin layer. Optical properties derived from UV-Vis analysis showed that CZTS has a direct band gap of 1.5 eV in the visible range which is close to typical values of an ideal absorber layer. Dielectric impedance measurements showed that CZTS thin film presents an adsorption in the lower frequencies of RF domain which is due to the atomic vibrations in the crystal lattice. The obtained CZTS has the potential to serve as a reliable, economical, and environment-friendly alternative to unstable, expensive and toxic absorber layers for photovoltaic applications.

Keywords: CZTS thin films, SILAR, Absorber layer, XRD, Kestrite.

DOI: [10.21272/jnep.15\(2\).02004](https://doi.org/10.21272/jnep.15(2).02004)

PACS numbers: 68.55.Nq, 81.15.-z, 42.79.Ek, 61.05.cp

1. INTRODUCTION

In recent years, considerable research effort has been devoted to producing effective, low-cost and earth-abundant innovative materials. This will remain the main focus for new studies of solar cell thin films. Different materials such as copper indium gallium selenide (CIGSe), Copper Indium Gallium Sulphur (CIGS), Copper Indium Sulphur (CuInS), Cadmium Telluride (CdTe) and kesterite have proved to be highly efficient for fabricating thin-film solar cells [1]. Although these solar cells show good photovoltaic properties, the materials used as absorbent layer contain toxic elements such as cadmium (Cd) and gallium (Ga) as well as some expensive elements such as tellurium (Te) and indium (In) [2]. Toxicity and expensiveness make these materials environmentally unsuitable and also unaffordable in the future [3]. In the past few decades, CZTS semiconductors have attracted the attention of the research community due to their wide range of applications in electronics, photocatalysis, energy storage devices, solar cells [4], etc. CZTS ($\text{Cu}_2\text{ZnSnS}_4$) is a quaternary semiconductor compound of group I-II-IV-VI which crystallizes in a structure that can be of the stannite or kesterite type [5]. Thin films of

CZTS are composed of abundant materials on earth with low toxicity (Copper (Cu), Zinc (Zn), Tin (Sn) and Sulfur (S)), and they have *p*-type conductivity, large band gap (in the range of 1.4-1.6 eV) with a high absorption coefficient (over 10^4 cm^{-1}) that make it an excellent and promising material for solar cells [6]. CZTS thin films can be prepared by various physicochemical methods such as pulsed laser deposition [7], electrochemical deposition [8], chemical bath deposition [9], spray pyrolysis [10] and spin coating [11], etc. However, some of these methods suffer from expensive hardware requirements and significant power consumption. In this study, CZTS films were formed using a homemade SILAR method in order to improve the growth process and reduce the production cost.

2. EXPERIMENTAL DETAILS

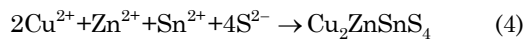
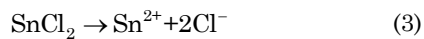
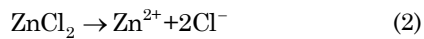
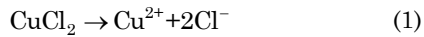
2.1 Elaboration of CZTS thin films

Glass substrates of 75 mm × 25 mm × 1 mm size were ultrasonically cleaned in four successive steps: 20 % HCl, acetone, ethanol, and finally deionized water, respectively. Each step lasted 20 min. After that, two solutions were prepared: cationic and anionic. The

* bouchra.benmazouza@univ-usto.dz

† djelloulertse@gmail.com

cationic solution was obtained by dissolving 0.02M CuCl₂, 0.05M ZnCl₂, 0.05M SnCl₂ in deionized water and the anionic one contained thiourea 0.04M CS(NH₂)₂. Few drops of ammonia were added to both solutions in order to ensure the adsorption on the glass substrate. Finally, the ultrasonically cleaned glasses were immersed in the cationic precursor solution and then in the anionic one with rinsing between each immersion in order to remove the precipitation. The adsorption and reaction times were fixed at 40 seconds and the rinsing time was about 30 seconds. The chemical reactions to form CZTS are:



The SILAR process for synthesizing CZTS thin films is depicted in Fig. 1.

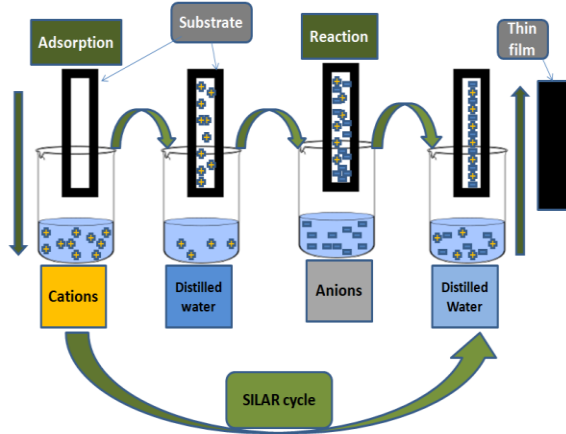


Fig. 1 – The SILAR process for synthesizing CZTS thin films

Fig. 2 shows the CZTS sample of (a) the as-deposited CZTS obtained in 100 cycles and (b) after 1 h of annealing in air. The obtained thin layers were adherent, smooth and uniform. The change of color from gray to dark black is due to the effect of heat treatment at 200 °C on the morphological properties [12].

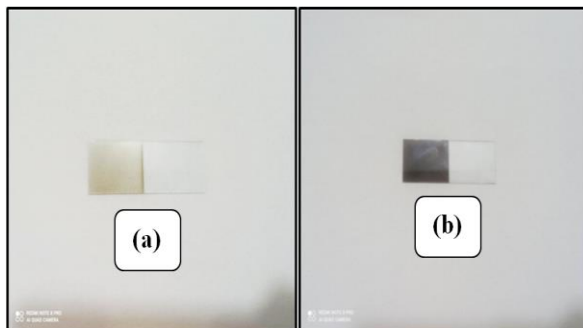


Fig. 2 – The CZTS thin films for 100 cycles (a) before annealing and (b) after annealing at 200 °C in air for 1 h

2.2 Characterization

The structural characterization of CZTS thin films was studied using an X-ray diffractometer (Panalytical

DY 1352) with CuK_α radiation ($\lambda = 1.54059 \text{ \AA}$) in angle 2θ in the range ($20^\circ \leq 2\theta \leq 90^\circ$). The Philips XL30 field-emission environmental scanning electron microscopy (FESEM) was used to study surface morphology. The two- and three-dimensional (2D and 3D) surface topography was investigated by the Atomic Force Microscope (AFM) in tapping mode by a JEOL model (JSPM 5200) with scanning areas of ($2 \mu\text{m} \times 2 \mu\text{m}$). The optical properties were observed by UV-Vis spectrophotometer (Cary 500) in the wavelength range of 350-1000 nm on glass substrates.

3. RESULTS AND DISCUSSION

3.1 Structural Properties

Fig. 3 shows the X-ray diffractogram of the CZTS sample after 1 h annealing at 200 °C in air atmosphere. All peaks correspond to the tetragonal structure of CZTS representing (110), (112), (200) and (312) crystal planes of pure tetragonal phase. It is a signature of the kesterite structure of the polycrystalline type which is known to be more stable than the stannite structure. Moreover, the CZTS have a preferential orientation according to the (112) crystal plane according to JCPDS 00-026-0575. The crystallite size was determined from Debye-Scherer's relation [13]:

$$D = \frac{k\lambda}{\beta \cos \theta} \quad (5)$$

Such as D is the crystallite size, k corresponds to Scherer constant, λ is the wavelength of X-rays (1.54059 Å), θ is the half of Bragg angle and β is the full width at half maximum (FWHM) of the peak. The lattice parameter and the crystallite size of the films are listed in Table 3. The results show that the average crystallite size is $\sim 102 \text{ \AA}$ which shows the formation of crystallites at nanometric scale at 200 °C annealing temperature.

The average crystallite size was found to be 102 Å. The diffraction study reveals that CZTS thin film has been formed with kesterite structure at an annealing temperature of 200 °C which is considerably lower than 470 and 575 °C reported by A. El Kissani et al. [14] and G.L. Agawane et al. [15], respectively. The obtained lattice parameters were $a = 5.443 \text{ \AA}$ and $c = 10.803 \text{ \AA}$. These values are in good agreement with reported lattice parameters $a = 5.427 \text{ \AA}$ and $c = 10.848 \text{ \AA}$ (JCPDS 00-026-0575 [16]).

3.2 Morphological Properties

The morphological characterizations were carried out using FESEM and AFM. Figure 4 shows SEM micrograph of the prepared CZTS thin film after annealing at 200 °C in air for 1 h. A quasi-uniform distribution of grains without any cracks was observed. The grains are well agglomerated all over the surface of the thin film. This is considered as a real advantage in photovoltaic conversion because it allows better collection of electrons and avoids losses by electron-hole recombination [17]. The empty areas located between the grains are due to the high number of cycles.

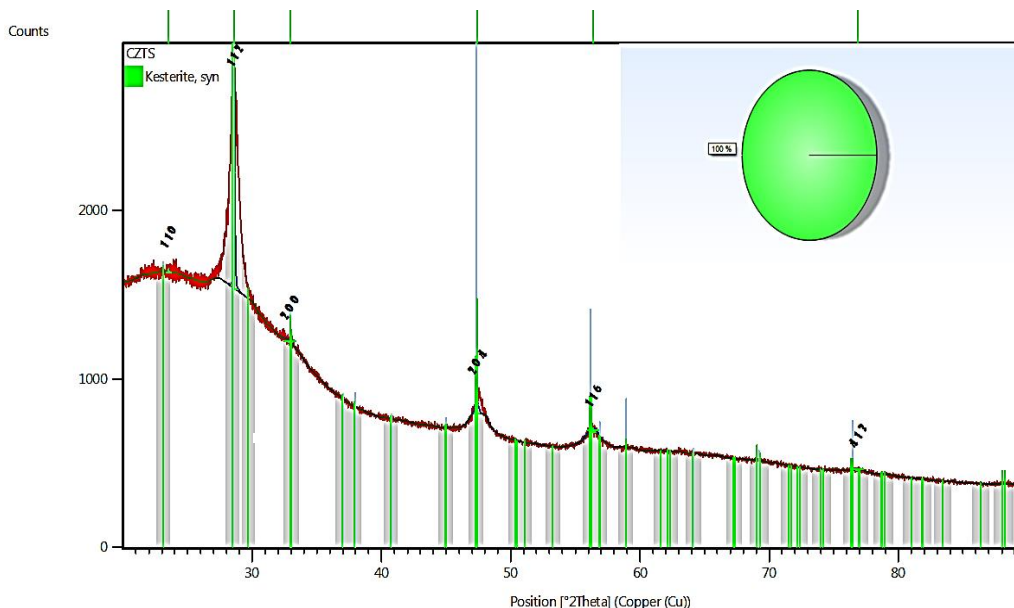


Fig. 3 – X-Ray diffraction pattern of CZTS thin film processed with the Philips HighScore Plus software

Table 1 – The structural parameter of CZTS thin film

Film	Crystallite size D (Å)	Lattice parameter a (Å)	Lattice parameter c (Å)	Volume V [Å ³]	Lattice strain (%)
CZTS	102	5.443	10.803	319.92	1.387
JCPDS 00-026-0575	–	5.427	10.848	319.50	–

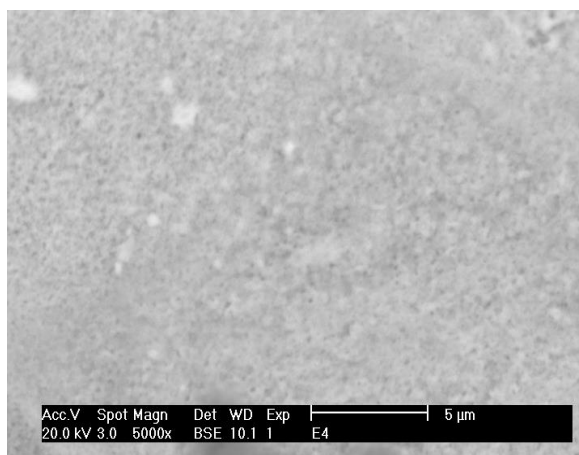


Fig. 4 – SEM micrograph of the CZTS thin film after annealing at 200 °C in air for 1 h

The AFM images of the CZTS sample represented in Fig. 5 show the presence of uniform spheres and nanowires all over the surface of the sample. The diameter of this nanowire is ~ 10 nm. Moreover, the thin film is smooth and free from cracks. This result is consistent with the previous SEM observations.

3.3 Optical properties

Fig. 6 shows the transmittance in the wavelength range (350-1000 nm) for the CZTS thin film after annealing at 200 °C in air for 1 h. Results show that the thin layer of CZTS produced using the SILAR method has a low average transmission ~ (24 %) situated in the visible range (400-800 nm), which is favorable for a thin absorber layer for photovoltaic application.

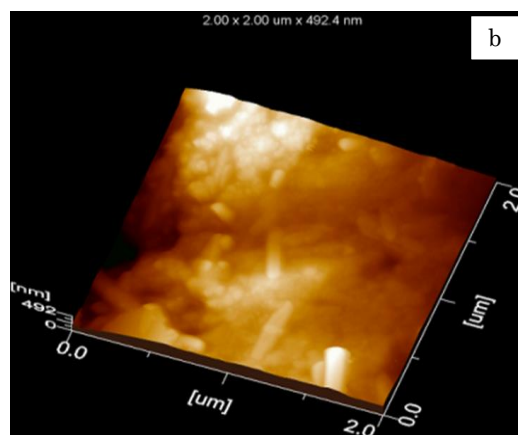
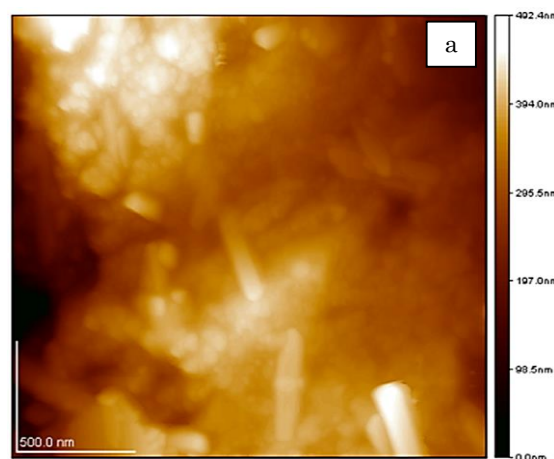


Fig. 5 – a) 2D and b) 3D AFM topographical images of CZTS thin film after annealing at 200 °C in air for 1 h

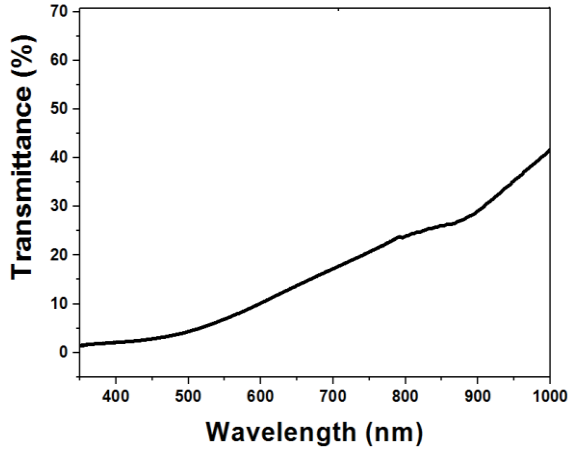


Fig. 6 – Transmittance of CZTS thin film

Fig. 7 shows the adsorption coefficient versus the wavelength (nm) in the visible range (400-800 nm). This parameter was calculated from the transmission data using the following equation [13]:

$$\alpha = \frac{-\ln(T)}{d} \tag{6}$$

Where α is the absorption coefficient, d corresponds to the thickness of the thin film and T is the transmittance. The obtained value of α is $\sim 1.6 \cdot 10^5 \text{ cm}^{-1}$. This result is very important for a p -type thin film absorber for photovoltaic applications.

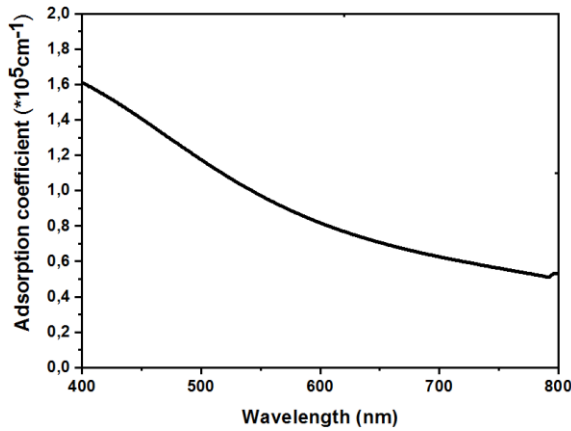


Fig. 7 – Adsorption coefficient of CZTS thin film

The plot of the curve from the variation of $(\alpha h\nu)^2$ as a function of $(h\nu)$ for a thin layer of CZTS shows that this material has a direct band gap. The extrapolated value from the linear part of the curve is $\sim 1.5 \text{ eV}$ (Fig. 8). According to the literature, the result obtained is in good agreement with typical gap values of CZTS [18].

3.4 Dielectric Properties

Fig. 9 depicts the real (ϵ') and imaginary (ϵ'') parts of dielectric permittivity of CZTS as a function of frequency. The imaginary dielectric constant (ϵ'') increases in the range (10^3 - 10^4 Hz). This correspond to the absorption of incident radiation and the setting of cations (Cu, Zn, Sn) and anions S vibration in the RF domain where the relation is [19]:

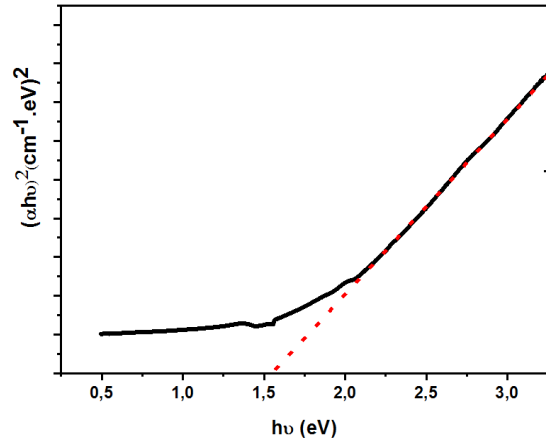


Fig. 8 – Band gap variation of CZTS

$$\alpha = \frac{4\pi k}{\lambda} \tag{7}$$

Where α represents the absorption coefficient, k corresponds to the extinction coefficient and λ is the wavelength. The real (ϵ') represents the reflection of incident radiation [20] where:

$$\epsilon' = i\epsilon'' \tag{8}$$

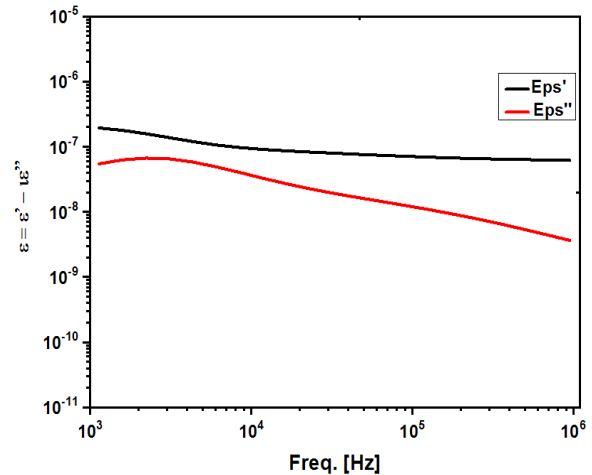


Fig. 9 – Dielectric permittivity of CZTS thin film

4. CONCLUSIONS

In this paper, CZTS absorber nanocrystalline thin film was successfully synthesized using SILAR method. 1 hour of annealing was sufficient to form a pure and single phase. XRD analysis confirm that the formation of CZTS in kesterite structure with an average crystallite size of 10.2 nm. SEM and AFM images show the homogeneity of the thin films free of cracks. A typical band gap of 1.5 eV was obtained by using UV-Visible spectrophotometry. The dialectical analysis shows an adsorption of incident radiation in the RF domain. The findings of this work confirm that homemade SILAR synthesized CZTS can be a reliable alternative to expensive and toxic absorber layers for photovoltaic applications.

ACKNOWLEDGEMENTS

This work was supported by the General Directorate for Scientific Research and Technological Development (Algerian Ministry of Higher Education and

Scientific Research). The authors wish to thank Dr. Omar Mosbah, member in LEPM laboratory for the help provided in order to have a high quality of dielectric analysis and Pr. Mokhetar Zerdali, member in LMESM for his help in the AFM characterization.

REFERENCES

1. C. Xiao, C.S. Jiang, M. Nardone, D. Albin, A. Danielson, A.H. Munshi, T. Shimpi, W. Sampath, S. Jones, M.M. Al-Jassim, G. Teeter, N.M. Haegel, H.R. Moutinho, *ACS Appl. Mater. Interfaces* **14** No 35, 39976 (2022).
2. X. Song, X. Ji, M. Li, W. Lin, X. Luo, H. Zhang, *Int. J. Photoenergy* **2014**, 1 (2014).
3. A. Krishnan, K. Rishad Ali, G. Vishnu, P. Kannan, *Mater. Renew. Sustain. Energy* **8** No 3, 16 (2019).
4. A. Murugan, V. Siva, A. S. Shameem, S.A. Bahadur, *J. Energy Storage* **44** 103423 (2021).
5. G.G. Silvena, B. John, R. Anne Sarah Christinal, M.C. Santhosh Kumar, S. Chakravarty, A. Leo Rajesh, *J. Inorg. Organomet. Polym. Mater.* **27** No 5, 1556 (2017).
6. S.A. Khalate, R.S. Kate, R.J. Deokate, *Sol. Energy* **15**, 616 (2018).
7. K. Moriya, K. Tanaka, H. Uchiki, *Jpn. J. Appl. Phys.* **47**, 602 (2008).
8. M. Jeon, T. Shimizu, S. Shingubara, *Mater. Lett.* **65**, 2364 (2011).
9. N.M. Shinde, C.D. Lokhande, J.H. Kim, J.H. Moon, *J. Photochem. Photobiol. A* **235**, 14 (2012).
10. N. Sebaa, M. Adnane, A. Djelloul, A. Abderrahmane, T. Sahraoui, *J. Nano-Electron. Phys.* **11** No 5, 05009 (2019).
11. C. Tamin, D. Chaumont, O. Heintz, et al., *Bol. Soc. Esp. Cerámica Vidr.* **60** No 6, 380 (2020).
12. A.A.H. El-Bassuony, *J. Inorg. Organomet. Polym. Mater.* **30** No 5, 1821 (2020).
13. A. Djelloul, M. Adnane, Y. Larbah, M. Zerdali, C. Zegadi, A. Messaoud, *J. Nano-Electron. Phys.* **8** No 2, 02005 (2016).
14. A. El Kissani, D. Ait El Haj, H. Ait Dads, F. Welatta, L. Nkhaili, K. El Assali, A. Outzourhit, *Spectroscopy Lett.* **53**, 123 (2019).
15. G.L. Agawane, A.S. Kamble, S.A. Vanalakar, S.W. Shin, M.G. Gang, Jae Ho Yun, Jihye Gwak, A.V. Moholkar, Jin Hyeok Kim, *Mater. Lett.* **158**, 58 (2015).
16. S. Ahmadi, N. Khemiri, A. Cantarero, M. Kanzari, *J. Alloy. Compd.* **925**, 166520 (2022).
17. S.M. Sze, Kwok K. Ng, *Physics and Properties of Semiconductors – A Review*, 5, In: *Physics of Semiconductor Devices* (John Wiley & Sons, Ltd: 2006).
18. S. Chamekh, N. Khemiri, M. Kanzari, *SN Appl. Sci.* **2**, 1507 (2020).
19. S. Zhu, T.P. Chen, Z.H. Cen, et al. *Opt. Exp.* **18** No 21, 21926 (2010).
20. K. Mauritz, *Dielectric Spectroscopy* (Mar 07, 2001 – Oct 06, 2014).

Розробка оптимізованого поглинаючого шару $\text{Cu}_2\text{ZnSnS}_4$, створеного SILAR методом

B. Benmazouza¹, T. Sahraoui¹, M. Adnane¹, N. Hamamousse², A. Djelloul³, Y. Larbah⁴, L. Benharrat³

¹ LMESM, Département de Technologie des Matériaux, Faculté de Physique, Université des Sciences et de la Technologie d'Oran Mohamed Boudiaf USTO-MB, BP 1505, El M'naouer, 31000 Oran Algérie

² LEPSM, Département de Technologie des Matériaux, Faculté de Physique, Université des Sciences et de la Technologie d'Oran Mohamed Boudiaf USTO-MB, BP 1505, El M'naouer, 31000 Oran Algérie

³ Centre de Recherche en Technologie des Semi-Conducteurs pour l'Energétique 'CRTSE', 02 Bd Frantz Fanon, BP 140, 7 Merveilles, Alger, Algérie

⁴ Spectrometry Department, Nuclear Research Center of Algiers-CRNA, 02 Bd. Frantz Fanon BP, 399 Algiers, Algeria

У цьому дослідженні тонкі плівки $\text{Cu}_2\text{ZnSnS}_4$ (CZTS) були синтезовані на скляних підкладках за допомогою саморобного методу адсорбції та реакції послідовного іонного шару (SILAR). Хлорид міді (II) (CuCl_2), хлорид цинку (II) (ZnCl_2), хлорид олова (II) (SnCl_2) використовували як катіонні прекурсори, а тиосечовину ($\text{CS}(\text{NH}_2)_2$) – як аніонні. Деіонізована (DI) вода була взята як розчинник для обох прекурсорів. До обох розчинів додавали кілька крапель аміаку, щоб забезпечити адсорбцію на скляній підкладці. Нанесені плівки були віддалені при 200 °C протягом 1 години в атмосфері повітря та досліджені методом рентгенівської дифракції (XRD), скануючої електронної мікроскопії (FESEM), атомно-силової мікроскопії (AFM), спектрофотометрії та діелектричної спектроскопії. Установлено утворення фази кестериту з переважною орієнтацією вздовж площини (112). Морфологічні спостереження за SEM та AFM показали рівномірний і однорідний тонкий шар CZTS. Оптичні властивості, отримані за допомогою аналізу УФ-видимого діапазону, показали, що CZTS має пряму заборонену зону 1,5 eV у видимому діапазоні, що є близьким до типових значень ідеального поглинаючого шару. Вимірювання діелектричного опору показали, що тонка плівка CZTS представляє адсорбцію на нижніх частотах радіочастотного домену, яка зумовлена атомними коливаннями в кристалічній решітці. Отриманий CZTS має потенціал, щоб служити надійною, економічною та екологічно чистою альтернативою нестабільним, дорогим і токсичним шарам поглиначів для фотоелектричних застосувань.

Ключові слова: Тонкі плівки CZTS, SILAR, Поглинаючий шар, XRD, Кестерит.